BIOCHEMISTRY
including biophysical chemistry & molecular biology

Article

pubs.acs.org/biochemistry

Age-Related Oxidative Modifications of Transthyretin Modulate Its Amyloidogenicity

Lei Zhao, Joel N. Buxbaum, and Natàlia Reixach*

Department of Molecular and Experimental Medicine, The Scripps Research Institute, 10550 North Torrey Pines Road, La Jolla, California 92037, United States

Supporting Information

ABSTRACT: The transthyretin amyloidoses are diseases of protein misfolding characterized by the extracellular deposition of fibrils and other aggregates of the homotetrameric protein transthyretin (TTR) in peripheral nerves, heart, and other tissues. Age is the major risk factor for the development of these diseases. We hypothesized that an age-associated increase in the level of protein oxidation could be involved in the onset of the senile forms of the TTR amyloidoses. To test this hypothesis, we have produced and characterized relevant age-related oxidative modifications of the wild type (WT) and the Val122Ile (V122I) TTR variant, both involved in cardiac TTR deposition in the elderly. Our studies show that methionine/cysteine-oxidized TTR and carbonylated TTR from either the WT or the V122I variant are thermodynamically less stable than their nonoxidized counterparts. Moreover, carbonylated WT and carbonylated V122I TTR have a stronger propensity to form aggregates and fibrils than WT and V122I TTR, respectively, at physiologically attainable pH values. It is well-known that TTR tetramer dissociation, the limiting step for aggregation and amyloid fibril formation, can be prevented by small molecules that bind the TTR tetramer interface. Here, we report that carbonylated WT TTR is less amenable to resveratrol-mediated tetramer stabilization than WT TTR. All the oxidized forms of TTR tested are cytotoxic to a human cardiomyocyte cell line known to be a target for cardiac-specific TTR variants. Overall, these studies demonstrate that age-related oxidative modifications of TTR can contribute to the onset of the senile forms of the TTR amyloidoses.

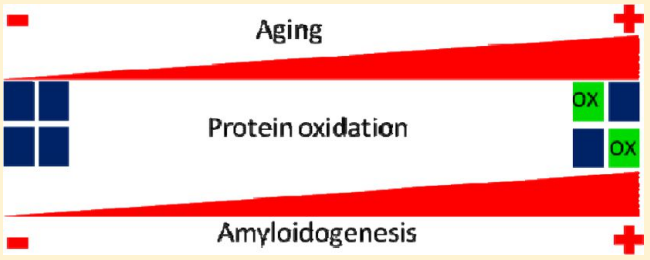

The amyloidoses are a subset of protein misfolding diseases characterized by the systemic extracellular deposition of β-sheet rich fibrils and amorphous aggregates in tissues that results in compromised organ function and death.[1] Transthyretin (TTR) is one of the ~30 human amyloidogenic proteins thus far identified.[2] TTR is a 55 kDa homotetramer synthesized mainly in the liver and the choroid plexus of the brain, which circulates in the plasma and the cerebrospinal fluid (CSF). The known functions of TTR are to transport retinol (through retinol-binding protein) and thyroxine (T_4) in plasma, and T_4 in the CSF. TTR can interact with a large variety of small molecules, including peptides such as amyloid β peptide,[3] suggesting that its function might also be that of a general detoxifier of unwanted molecules and metabolic byproducts.[4]

Wild-type (WT) TTR undergoes age-dependent deposition in the heart, gut, carpal tunnel, and lungs, producing the syndrome known as senile systemic amyloidosis (SSA). The average age of onset of SSA is 65−70 years, depending on the population studied.[5,6] Autopsy data indicate that 10−25% of people older than 80 are affected by WT TTR-derived amyloidosis, and it appears to be the cause of death of 10% of those older than 90 years.[5] There are more than 100 amyloidogenic TTR variants that have been associated with various protein deposition syndromes. Val122Ile (V122I) TTR is the most common amyloidogenic mutation worldwide. It produces the syndrome known as familial amyloid cardiomyopathy (FAC), characterized by age-dependent cardiac amyloid deposition resulting in arrhythmias, congestive heart failure, and death. The age of onset of FAC due to the V122I TTR mutant is approximately a decade earlier than that of WT TTR amyloidosis. Three to four percent of African-Americans are heterozygous for the V122I TTR allele, which produces clinical disease in almost 100% of the carriers.[7−9]

Biophysical studies have shown that the loss of TTR quaternary structure, i.e., the disassembly of the native tetramer into its constituent monomers, is required and is the rate-limiting step for aggregation and subsequent fibril formation in vitro, and presumably in vivo.[10] The released monomer misfolds and forms oligomers, soluble aggregates, insoluble aggregates, and amyloid fibrils in a downhill polymerization process.[11] Many of the amyloidogenic TTR variants studied thus far have lower thermodynamic and/or kinetic stabilities than WT TTR, which make the proteins more prone to tetramer disassembly, misfolding, and aggregation.[12,13]

Although it is well documented that age is the major risk factor for the development of TTR-associated diseases, it is not

Received: September 26, 2012
Revised: January 18, 2013
Published: February 15, 2013

dx.doi.org/10.1021/bi301313b | *Biochemistry* 2013, 52, 1913−1926

known which aspects of the aging process contribute to the onset of disease. Given the well-established general increase in the level of protein oxidation with aging,[14] we sought to investigate whether oxidative modifications in TTR might change its stability, increasing its tendency toward aggregation and fibril formation.

There are several types of oxidative modifications that occur in proteins. Sulfur-containing amino acids such as methionine (Met) and cysteine (Cys) are some of the most susceptible to oxidation.[15] The addition of one oxygen atom into the sulfur of Met generates methionine sulfoxide (MetO). Cys oxidation results in the formation of disulfide bonds and Cys sulfenic, sulfinic, and sulfonic acids by addition of one, two, and three oxygen atoms, respectively.[16,17] Both Met and Cys oxidation processes are reversible and have biological as well as pathological significance.[18,19] Another type of age-related oxidative modification is protein carbonylation, which results in the formation of reactive aldehydes and ketones by a variety of mechanisms.[14] Lys, Arg, Pro, and Thr residues, for example, are susceptible to metal-catalyzed carbonylation of their side chains.[20] Protein carbonylation is common, irreversible, and considered to be a universal indicator of oxidative stress or damage.[21] It has been established that the content of carbonylated proteins increases dramatically in the last third of life,[22] and it is highly correlated with age-related diseases such as Alzheimer's[23,24] or Parkinson's disease.[25] Carbonylated TTR has been identified in human plasma of healthy individuals[26,27] as well as in CSF.[28] Furthermore, an increase in the level of protein carbonyls has been reported in biopsies of patients with TTR deposits compared to age-matched controls,[29] although it is not clear from this report whether TTR itself is carbonylated.

Previously, we showed that H_2O_2-induced oxidation of WT TTR and the amyloidogenic variant Val30Met (V30M) TTR results in proteins with lower propensities to form aggregates and fibrils at pH 4.4 as measured by turbidity.[30] In the study presented here, we have produced and characterized relevant age-related oxidized TTR isoforms. We demonstrate that treatment of WT and V122I TTR with H_2O_2 results in the transformation of all Met and Cys residues into MetO and Cys sulfonic acid (Cys-SO_3H). In addition, we have prepared carbonylated WT and V122I TTR. Aggregation and fibril formation studies at several pH values confirm our previous work with respect to H_2O_2-oxidized WT TTR at pH 4.4. More interestingly, the data show that the oxidized TTR isoforms, particularly carbonylated TTRs, form more insoluble aggregates at pH values closer to physiological conditions than their nonoxidized counterparts. Moreover, urea denaturation−renaturation studies show that the oxidative modifications render the TTR tetramers thermodynamically less stable than the nonoxidized isoforms. Transgenic mouse models and human biopsies of asymptomatic TTR mutant carriers have shown evidence of tissue damage and cell death well before there is detectable TTR deposition.[31] Here, we demonstrate that the oxidized TTR isoforms are cytotoxic to human cardiomyocytes in a tissue culture model that reflects the specificity of cardiac TTR variants.[32] On the whole, the data reveal that age-related TTR oxidative modifications can play a role in the onset of the senile forms of the TTR amyloidoses.

EXPERIMENTAL PROCEDURES

Recombinant Protein Preparation. TTR variants were prepared and purified in an *Escherichia coli* expression system as described previously.[33] The last step of purification was gel filtration chromatography on a Superdex 75 column (GE Healthcare) in sodium phosphate buffer {GF buffer [10 mM sodium phosphate (pH 7.6), 100 mM KCl, and 1 mM EDTA]} or Hank's Balanced Salt Solution (HBSS) (Mediatech, Manassas, VA) without phenol red. Additional recombinant TTR variants (named rTTRs) were produced using the published vector and protocols from L. Connors' laboratory to produce His-tagged TTR.[34] During purification, the His tag is cleaved by dipeptidyl aminopeptidase I (Qiagen) yielding TTR lacking Met at position-1. Site-directed mutagenesis was used to create C10A TTR, M13I TTR, C10A rTTR, and M13I rTTR. The plasmids obtained were sequenced to confirm that we had introduced the desired point mutations. The identity of the proteins was determined by liquid chromatography-mass spectrometry (LC−MS). The molecular masses of the variants were 13892 Da for WT TTR, 13907 Da for V122I TTR, 13860 Da for C10A TTR, 13874 Da for M13I TTR, 13923 Da for T119M TTR, 13894 Da for F87M/L110M TTR, 13760 Da for rTTR, 13728 Da for C10A rTTR, and 13742 Da for M13I rTTR. All TTR proteins were stored as aliquots at −80 °C at concentrations of <2.5 mg/mL. Under these conditions, we observed no changes in oxidation or aggregation of the proteins over time.

H_2O_2 Oxidation. TTR variants (1.5−2.5 mg/mL in GF buffer) were treated with 3% hydrogen peroxide (H_2O_2, H1009, Sigma-Aldrich) at room temperature for 30 min. The concentration of the H_2O_2 stock solution was regularly measured by spectrophotometry (ε_{240} = 43.6 M^{-1} cm^{-1} [35]). The oxidized TTRs were then purified by gel filtration on a Superdex 75 column to remove the excess oxidant and any TTR aggregates generated during the oxidative reaction. LC−MS analysis consistently revealed a single species with a molecular mass corresponding to the complete transformation of all Met residues into Met sulfoxide (MetO) and the oxidation of the single Cys residue at position 10 to Cys sulfonic acid (Cys-SO_3H) (see Results).

Iron-Catalyzed Carbonylation. TTR carbonylation was performed as described in ref 36. Briefly, WT or V122I TTR (10 mg/mL) was dialyzed against 25 mM Hepes (pH 7.4), 100 mM KCl, and 10 mM $MgCl_2$ and then incubated in freshly prepared oxidative reaction buffer [25 mM sodium ascorbate, 100 μM $FeCl_3$, solubilized in 25 mM Hepes (pH 7.4), 100 mM KCl, and 10 mM $MgCl_2$] at 37 °C for 5 h or overnight. The proteins were repurified by gel filtration to remove excess reagents and TTR aggregates. The presence of the newly generated carbonyl groups was confirmed using the Oxyblot protein oxidation detection kit (S7150, Millipore). Briefly, the proteins were derivatized with dinitrophenylhydrazine, separated by sodium dodecyl sulfate−polyacrylamide gel electrophoresis, and transferred onto a PVDF membrane. The derivatized proteins were detected using a rabbit anti-diphenylhydrazone antibody (1:150) or a rabbit anti-human TTR antibody (A0002, Dako) followed by alkaline phosphatase-labeled goat anti-rabbit IgG (A-8025, Sigma-Aldrich).

Far- and Near-UV Circular Dichroism (CD). The far- and near-UV CD spectra of native WT and V122I TTR and their oxidized isoforms (8 μM in GF buffer) were acquired at 25 °C using an AVIV 202SF CD spectrometer (AVIV, Lakewood, NJ) equipped with a Peltier thermostated cell holder. Far-UV CD spectra were recorded from 190 to 250 nm using a 2 mm path length Suprasil quartz cell with a 1 nm bandwidth; Figure S2 of the Supporting Information shows the spectra from 205 to 250

nm to omit the noise due to the buffer absorbance at lower wavelengths. Near-UV CD spectra were recorded from 250 to 320 nm in a 1 cm path length quartz cell with a 1 nm bandwidth. The wavelength step was set at 0.5 nm with time constants of 100 ms for both far- and near-UV CD. Blank spectra corresponding to GF buffer were subtracted from the samples, and the data were transformed to mean residue ellipticity, θ_{MRW} (degrees square centimeters per decimole). Each spectrum represents the average of four scans. No smoothing algorithm was applied to any of the spectra to conserve detail.

Acid-Mediated TTR Aggregation and Fibril Formation. pH-dependent fibril formation studies were performed as described previously.[37] Briefly, TTR solutions in GF buffer (8 μM, ~0.4 mg/mL) were diluted 1:1 with acidic buffers (200 mM sodium citrate, acetate, or phosphate with 100 mM KCl and 1 mM EDTA) to achieve various pH values (4.04−5.88). The mixtures were incubated at 37 °C for the desired amount of time (up to 21 days) in cluster tubes (Genessee Scientific, San Diego, CA). At the end of the incubation time, the TTR solutions were vortexed for 10 s and transferred into $^1/_2$ area 96-well UV-transparent plates (Corning) in triplicate (50 μL/well). The turbidity of the solutions at 400 nm was recorded using a UV spectrophotometer (SpectramaxPlus, Molecular Devices). Blanks consisting of the corresponding buffer solutions were subtracted from each sample. All experiments were repeated at least twice in triplicate.

Measurement of Amounts of Soluble and Insoluble TTR. Samples of 400 μL of aggregated TTR solutions (see above) were transferred into fresh Eppendorf tubes and centrifuged at 20000*g* for 30 min at 4 °C. The supernatants were carefully transferred into fresh Eppendorf tubes, and the protein concentration in these solutions was measured using $^1/_2$ area 96-well UV-transparent plates in triplicate (50 μL/well). To determine the amount of aggregated TTR (insoluble), 200 μL of an 8 M guanidinium chloride (GndCl) solution was added to the protein precipitates. The samples were then vortexed briefly and left at room temperature for 5 min to allow the disassembly of TTR aggregates to take place. The TTR concentration was then measured by UV spectrophotometry in $^1/_2$ area 96-well UV-transparent plates in triplicate, using 8 M GndCl as a blank. The percentages of protein in the supernatant and pellet were calculated from the total initial protein content at time zero.

Inhibition of TTR Aggregation and Fibril Formation by Resveratrol. TTR solutions (8 μM, 250 μL) in GF buffer were added to 1 μL of resveratrol (4 mM stock in DMSO, 2 equiv of resveratrol/TTR) or to 1 μL of DMSO (vehicle control). The samples were vortexed and incubated at room temperature for 30 min to allow resveratrol binding. Two hundred and fifty microliters of acetate buffer [200 mM sodium acetate (pH 4.23), 100 mM KCl, and 1 mM EDTA] was added to achieve a final pH of 4.4. The mixtures were incubated at 37 °C for 3 days. The samples were centrifuged at 20000*g* for 30 min at 4 °C, and the aggregated TTR was measured as described above using 8 M GndCl. The percentage of insoluble TTR in the samples containing resveratrol was calculated relative to that in the samples containing TTR alone (with DMSO).

Thioflavin T (ThT) Binding. TTR aggregation and fibril formation were performed as described above for 1 or 3 days at a final pH of 4.4. The solutions were then diluted to 1 μM (tetramer equivalent) in 200 mM Tris and 150 mM NaCl (pH 8.0). Two microliters of a ThT stock solution [2 mM in 200 mM Tris and 150 mM NaCl (pH 8.0)] was added to 400 μL of the diluted TTR aggregates. The samples were vortexed briefly and dispensed into black 96-well plates (Corning) in triplicate (100 μL/well), and the ThT fluorescence was recorded with excitation and emission wavelengths of 440 and 482 nm, respectively, and a 5 nm bandwidth using a multiwell spectrofluorimeter (Tecan Safire 2).

Transmission Electron Microscopy (TEM). Carbon-coated copper grids (400 mesh, Electron Microscopy Sciences, Hatfield, PA) were glow-discharged and inverted on 5 μL aliquots of TTR subjected to acid-mediated aggregation conditions (final protein concentration of 4 μM, pH 4.4, 1 day at 37 °C) for 2 min. Excess sample was removed, and the grids were immediately placed briefly on a droplet of 0.1% ammonium acetate followed by a 2% uranyl acetate solution for 2 min. Excess stain was removed, and the grids were allowed to thoroughly dry. Grids were then examined on a Philips CM100 electron microscope (FEI, Hillsbrough, OR) at 80 kV and images collected using a Megaview III CCD camera (Olympus Soft Imaging Solutions, Lakewood, CO).

Urea Stability. TTR denaturation curves were prepared by incubating TTR at 0.1 mg/mL (~2 μM) in various concentrations of urea (range 0−8 M) in sodium phosphate buffer [50 mM sodium phosphate, 100 mM KCl, and 1 mM EDTA (pH 7.6)] for 4 days at room temperature. For the renaturation curves, TTR was first denatured in 6.5 M GndCl overnight at room temperature, then buffer exchanged into 8 M urea, and concentrated to 1 mg/mL. Dilutions were prepared to yield a final TTR concentration of 0.1 mg/mL over a wide range of urea concentrations (1−8 M) and were incubated for 24 h at room temperature before measurement of the tertiary and quaternary structures.

Determination of the Tertiary Structure by Tryptophan Fluorescence. The stability of the TTR tertiary structure was determined by measuring the intrinsic tryptophan fluorescence of the protein in the presence of urea, as described in ref 37. At the time of measurement, the samples were vortexed and transferred into $^1/_2$ area black 96-well plates (Corning) in triplicate (50 μL/well), and the tryptophan fluorescence was measured with an excitation wavelength of 295 nm and emission wavelengths of 335 and 355 nm, with a 10 nm bandwidth. The percentage of folded protein at each urea concentration was calculated from the fluorescent ratio values (355 nm to 335 nm) with respect to TTR samples that had not been denatured (100% folded) and those that were completely unfolded (0% folded). The data were fit to sigmoidal curves with variable slopes using GraphPad Prism (GraphPad, San Diego, CA), and the concentration of urea at which 50% of the TTR was folded (C_m) was calculated. For kinetic studies, TTRs were incubated in 6 M urea, a concentration in the post-transition region for tertiary structural changes. The tryptophan fluorescence was measured over time as described above. To assess tertiary structural changes of the oxidized proteins with respect to their nonoxidized counterparts, tryptophan emission spectra from nondenatured TTRs (4 μM in GF buffer) were also acquired using an excitation wavelength of 295 nm and an emission wavelength range from 320 to 400 nm with 1 nm steps.

Determination of the Quaternary Structure by Resveratrol Binding Fluorescence. The small molecule resveratrol binds in the T_4 binding pocket of tetrameric TTR, resulting in an increase in the fluorescence quantum yield. The

intensity of resveratrol fluorescence is proportional to the concentration of tetrameric TTR in solution.[37] To determine the amount of tetrameric TTR present in each of the urea solutions, 4 μL of resveratrol (1 mM in DMSO) was added to 200 μL of the TTR samples in urea. The resveratrol/TTR mixtures were vortexed briefly and incubated for 30 min at room temperature. Aliquots of 50 μL were then transferred into $^1/_2$ area black 96-well plates in triplicate, and the resveratrol fluorescence was recorded (excitation and emission wavelengths of 320 and 394 nm, respectively, with a 10 nm bandwidth). The proportion of tetrameric protein at each urea concentration was calculated using the average fluorescence values of TTR at very low urea concentrations (0−2 M) (100% tetramer) and the average fluorescent values of completely denatured TTR (0% tetramer). The data were fit to sigmoidal curves with variable slopes using GraphPad Prism, and the concentration of urea at which 50% of TTR is tetrameric (C_m) was calculated.

Cell Culture. The human cardiomyocyte cell line AC16[38] was routinely cultured in DMEM/F12 (Mediatech) supplemented with 10% FBS, 1 mM Hepes, 2 mM L-glutamine, 100 units/mL penicillin, and 100 μg/mL streptomycin and incubated at 37 °C in a 5% CO_2 environment.

Cytotoxicity Assessment. Subconfluent AC16 cells were seeded into black wall clear bottom 96-well plates (Corning) in Opti-MEM (Invitrogen, San Diego, CA) supplemented with 5% FBS, 1 mM Hepes, 2 mM L-glutamine, 100 units/mL penicillin, and 100 μg/mL streptomycin and incubated overnight. The next day, the culture medium was removed and the cells were exposed to different concentrations of TTR (100 μL) in a 1:1 Opti-MEM/HBSS mixture supplemented with 0.4 mg/mL BSA, 1 mM Hepes, 2 mM L-glutamine, 100 units/mL penicillin, 100 μg/mL streptomycin, and 4.5 mM $CaCl_2$. Cytotoxicity was determined by the resazurin assay after the samples had been treated for 24 h as previously described.[32] Briefly, 10 μL of resazurin solution (500 μM in PBS) per well was added, and the cells were incubated for 2.5 h at 37 °C. The fluorescence resulting from the reduction of resazurin to resorufin by metabolically active cells was measured using excitation and emission wavelengths of 530 and 590 nm, respectively, with a 10 nm bandwidth. Cell viability was calculated as the percentage of fluorescence of treated cells with respect to the control cells (vehicle-treated cells), after subtraction of the blank (wells with no cells). All experiments were repeated at least twice in triplicate. Averages and the standard error of the mean are presented.

RESULTS

TTR Methionine and Cysteine Residues Are Oxidized by H_2O_2. WT TTR and V122I TTR were treated with 3% H_2O_2 as detailed in Experimental Procedures. LC−MS analysis showed 100% conversion to a single product with a molecular mass 80 Da above that of the nonoxidized proteins, indicating that each TTR polypeptide chain had incorporated five oxygen atoms (Table 1).

The sulfur atoms of Met and Cys are the most susceptible to oxidation by ROS.[39] Met oxidation can generate two oxidative products, MetO or Met sulfone, by addition of one or two oxygen atoms, respectively.[16] Cys oxidation can result in Cys sulfenic, sulfinic, or sulfonic acid derivatives by incorporation of one, two, or three oxygen atoms, respectively.[16,17]

LC−tandem mass spectrometry (LC−MS/MS) analysis of native WT TTR showed oxidation at Met13 due to sample manipulation before analysis (alkylation and trypsinization); therefore, we could not use this technique to determine where oxidation took place in the H_2O_2-treated TTRs (not shown). Thus, we prepared and purified several recombinant TTR variants containing different numbers of Met or Cys residues in the sequence. These variants were treated with H_2O_2 and analyzed by LC−MS as described above (Table 1). H_2O_2-treated WT TTR incorporated five oxygen atoms, whereas C10A TTR incorporated two oxygen atoms. These results suggest that upon H_2O_2 treatment Cys is oxidized to Cys-SO_3H. Substitution of a Met residue in the sequence (M13I TTR) resulted in the incorporation of four oxygen atoms (one less oxygen atom than WT TTR), whereas addition of one and two Met residues (T119M TTR and F87M/L110M TTR, respectively) resulted in the incorporation of six and seven oxygen atoms, respectively. These results indicate that Met is oxidized to MetO (i.e., one oxygen atom per Met).

Table 1. Mass Spectrometry Analysis of Several TTR Variants Subjected to H_2O_2 Oxidation[a]

	no. of Met residues	no. of Cys residues	increase in molecular mass (Da)	no. of oxygen atoms
WT	2	1	80	5
V122I	2	1	80	5
C10A	2	0	32	2
M13I	1	1	64	4
T119M	3	1	96	6
F87M/L110M	4	1	112	7
rTTR[b]	1	1	64	4
M13I rTTR	0	1	48	3
C10A rTTR	1	0	16	1

[a]Shown are the number of Met and Cys residues in the sequences, the increase in molecular mass observed after H_2O_2 treatment with respect to native (nonoxidized) TTR, and the number oxygen atoms equivalent to the observed change in molecular mass. The TTR variants differ in only the number of Met and Cys residues in the sequence. [b]rTTR is recombinant protein lacking Met at position −1.[34]

To further confirm our results, we used a plasmid that after expression and purification produces TTR lacking Met at position −1, named rTTR.[34] We used site-directed mutagenesis to prepare variants of this rTTR and study their susceptibility to H_2O_2 oxidation as described above (Table 1). Treatment of rTTR and M13I rTTR with H_2O_2 resulted in the incorporation of four and three oxygen atoms, respectively, whereas C10A rTTR incorporated only one oxygen atom. Taken together, these results indicate that under our experimental conditions, H_2O_2 treatment of TTR results in the oxidation of all Met to MetO and Cys to Cys-SO_3H. These Met/Cys-oxidized TTRs are named oxi-TTRs in the text.

TTR Carbonylation in Vitro Results in Multiple Oxidative Products. WT and V122I TTR oxidative carbonylation was performed as described in ref 36. The presence of TTR carbonyls was confirmed by Oxyblot technology (Figure S1 of the Supporting Information). Carbonylated WT and V122I TTR were further analyzed by LC−MS. Thirty four percent of WT and 18% of V122I TTR were carbonylated after reaction for 5 h, whereas 100% of the proteins were carbonylated after overnight reaction. In all cases, a large number of oxidative products were detected, consistent with the fact that there are 32 amino acid residues in the TTR sequence that are susceptible to direct oxidative carbonylation.[36] The carbonylated TTRs were named car-TTRs. For

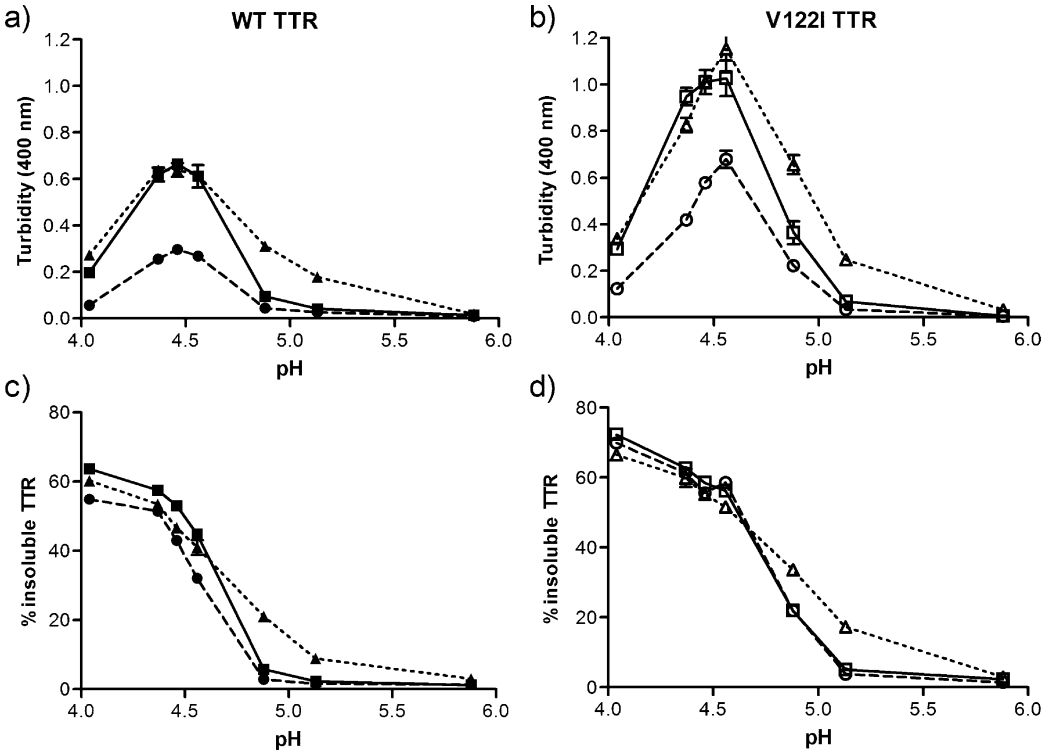

Figure 1. pH-dependent aggregation of native and oxidized TTRs. WT (a and c) and V122I TTR (b and d) and their oxidized isoforms (oxi-TTRs and car-TTRs) were incubated for 7 days at the designated pH at 37 °C. The extent of aggregation was measured by turbidity at 400 nm (a and b) and percentage of insoluble protein with respect to initial protein content (c and d): native TTR (solid line, squares), oxi-TTR (dashed line, circles), and car-TTR (dotted line, triangles). Data for WT TTR and its isoforms are represented by filled symbols; data for V122I TTR and its oxidized isoforms are represented by empty symbols. Data are shown for one representative experiment performed in triplicate (mean ± SD).

the aggregation and stability studies described below, we used the 5 h carbonylation products of WT and V122I TTRs as mixtures without trying to purify any specific carbonylation species because, when TTR carbonylation occurs in vivo, it is very likely that complex mixtures, and not a single carbonylation product, are generated.

The Secondary and Tertiary Structures of TTR and Its Oxidized Isoforms Are Similar. Far-UV CD (secondary structure) and near-UV CD as well as tryptophan fluorescence spectra (tertiary structure) were recorded for WT and its oxidized isoforms (oxi-WT and car-WT TTR) as well as for V122I TTR and its oxidized isoforms (oxi-V122I and car-V22I TTR). The far- and near-UV CD data show no major differences in the spectra (Figure S2 of the Supporting Information) of the oxidized TTRs (oxi- and car-TTRs) with respect to their nonoxidized counterparts. The tryptophan emission spectra are identical for WT and oxi-WT as well as for V122I and oxi-V122I TTR. The carbonylated proteins, however, have lower maximal fluorescence intensity than nonoxidized or oxi-TTRs. These differences are not unexpected because of the multiple amino acid residues that are susceptible to carbonylation in the TTR sequence,[32] some of which may be spatially close to the two tryptophan residues (Trp41 and Trp79) of the molecule. For TTR, a shift in the maximal emission wavelength from 335 to 355 nm is indicative of TTR unfolding.[40] The maximal emission wavelength for the three isoforms (nonoxidized, oxi-TTR, and car-TTR) is the same (335 nm), suggesting that they are all properly folded (Figure S2 of the Supporting Information).

What Is the Relationship of Sample Turbidity to TTR Aggregation and Thioflavin T Binding? TTR aggregation can be induced in vitro under mildly acidic conditions, and its extent can be monitored by recording the turbidity at 330−400 nm using UV−vis spectrophotometry.[12,41] Native WT and V122I TTR and their oxidized variants (oxi-TTRs and car-TTRs) were incubated from pH 4.04 to 5.88 for up to 7 days at 37 °C without agitation, and the extent of aggregation was measured by the turbidity at 400 nm (Figure 1). To determine whether turbidity was a measure of aggregation in these highly modified proteins, we also measured the total amount of aggregated (insoluble) protein and the amount of protein remaining in the supernatant. Similar aggregation studies were also performed with shorter (hours) and longer (up to 21 days) incubation times at pH 4.4, the pH of maximal turbidity for WT and V122I TTR[42] (Figure S3 of the Supporting Information). The results show that turbidity does not quantitatively represent aggregated protein (insoluble). At pH 4.04, for example, all the samples have very low turbidity (Figure 1a,b), while it is at this pH where we found the most aggregated (insoluble) TTR (Figure 1c,d). This inconsistency is also observed in the longer kinetic experiments at pH 4.4 where the turbidity of WT TTR and car-WT TTR increases steadily from 3 to 21 days, but the amount of insoluble protein recovered remains constant (Figure S3a,b of the Supporting Information). Moreover, for oxi-WT TTR and oxi-V122I TTR, the maximal turbidity values (pH 4.37−4.56) are approximately half of the values obtained for their nonoxidized counterparts (WT and V122I TTR) (Figure 1a,b), whereas the amount of insoluble protein is slightly lower in oxi-WT than in WT TTR (Figure 1c) and is the same in V122I and oxi-V122I TTR (Figure 1d). The percentages of protein remaining in the supernatants after centrifugation are complementary to those found in the pellets

dx.doi.org/10.1021/bi301313b | *Biochemistry* 2013, 52, 1913−1926

(not shown). Studies similar to those reported in Figure 1 in which the TTR aggregation reactions were analyzed after incubation for 1 and 3 days at 37 °C gave the same relative patterns of aggregation with respect to the turbidity and amount of insoluble protein recovered as those shown in Figure 1 (pH-dependent aggregation, 7 days) and Figure S3 of the Supporting Information (time-dependent aggregation, pH 4.4).

We used thioflavin T (ThT) binding fluorescence as an additional method to quantify TTR aggregation and fibril formation in vitro.[43] Native and oxidized TTRs were incubated with acidic buffer (pH 4.4) at 37 °C for 1 and 3 days without agitation. ThT fluorescence, the percentage of precipitated protein, and turbidity at 400 nm were measured as detailed in Experimental Procedures. The results shown in Figure 2 (incubation for 3 days) are presented as percentages relative to native TTRs. The data show that the percentage of ThT fluorescence (white bars) is similar to that of precipitated protein (black bars) for each TTR variant. The same correlation was seen for samples incubated for 1 day at 37 °C, as well as for samples incubated at pH 4.04 for up to 7 days (not shown).

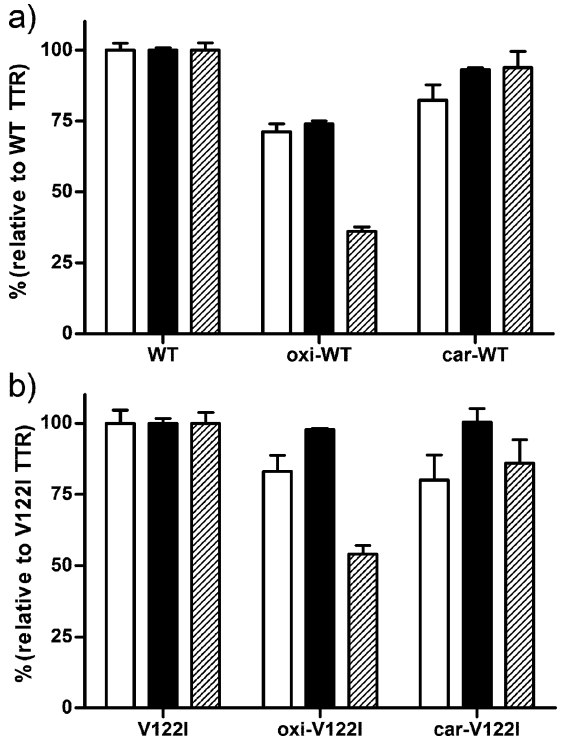

Figure 2. Relative aggregation of WT TTR (a) and V122I TTR (b) and their oxidized isoforms. TTR aggregates and fibrils were generated by incubation at pH 4.4 for 3 days at 37 °C. The extent of aggregation was measured by thioflavin T fluorescence (white bars), the percentage of insoluble protein with respect to initial protein content (black bars), and turbidity at 400 nm (hatched bars). All the values were normalized to those resulting from nonoxidized WT TTR and V122I TTR. The results shown represent the average of three independent experiments (mean ± SD).

Given that turbidity does not reflect the amount of aggregated (insoluble) protein under all conditions or with all the TTR variants, we will refer to protein aggregation as the percentage of precipitated protein after the designated incubation times.

Oxidation Modifies TTR Aggregation Propensity. Figure 1 shows that oxi-WT TTR aggregates slightly less than WT TTR whereas oxi-V122I TTR aggregates to the same extent as V122I TTR. The kinetic aggregation data show that at pH 4.4 both oxi-WT TTR and oxi-V122I TTR aggregate more slowly than WT and V122I TTR, respectively, although the end points of aggregation are similar (Figure S3 of the Supporting Information). More interestingly, at pH 4.88 and 5.13, car-WT and car-V122I TTR form more aggregates than nonoxidized WT and V122I TTR, respectively. The differences are particularly significant for car-WT TTR (~21% aggregated protein at pH 4.88) relative to WT TTR (~9% aggregated protein at pH 4.88). These findings are relevant because they indicate that in vivo car-WT and car-V122I TTR can aggregate at a pH closer to physiological conditions and, hence, potentially initiate the senile forms of the TTR amyloid diseases.

Monomeric Oxi-TTR Aggregates More Slowly Than Monomeric TTR. The aggregation experiments show that oxi-TTRs aggregate at a slower rate than their nonoxidized counterparts (Figure S3 of the Supporting Information). To assess whether the decreased rate of aggregation comes exclusively from the tetramers or whether the monomeric subunits are also less prone to aggregation, we performed fibril formation kinetic studies at pH 4.4 using the well-characterized monomeric TTR variant designated M-TTR (F87M/L110M TTR)[44] and its oxidized isoforms (named oxi-M-TTR and car-M-TTR). M-TTR has the same tertiary structure as each of the subunits of native TTR (WT TTR), but the Met residues introduced at the dimer−dimer interfaces (positions 87 and 110) prevent its tetramerization by steric hindrance. LC−MS analysis of H_2O_2-treated M-TTR indicated that all the Met residues in the sequence had gained one oxygen atom (Met to MetO transformation) and Cys10 became Cys-SO_3H (Table 1). Carbonylation of M-TTR (reaction for 5 h) was confirmed by Oxyblot (Millipore) and LC−MS. The yield of carbonylation was 42% (not shown). The aggregation and fibril formation data show that oxi-M-TTR aggregates more slowly (measured as insoluble protein) than M-TTR (Figure 3), whereas car-M-TTR and M-TTR aggregate at a similar rate. After incubation for 2 days at 37 °C, both oxi-M-TTR and car-M-TTR aggregated almost to the same extent as M-TTR did.

Inhibition of Aggregation by Resveratrol Is Less Effective for Carbonylated WT TTR Than for Non-oxidized WT TTR. Resveratrol is a polyphenolic compound known to kinetically stabilize tetrameric TTR by binding in its T_4 pocket and thus preventing TTR aggregation and fibril formation in vitro, and TTR-induced cytotoxicity in tissue culture.[32,33,45] Native and oxidized WT samples were incubated for 3 days at pH 4.4 with or without 2 equiv of resveratrol. Aggregation was measured as the percentage of insoluble protein formation (Figure 4). The data show that WT and oxi-WT TTR aggregation and fibril formation can be effectively inhibited by resveratrol (>94 ± 0.8% aggregation inhibition with respect to TTR without resveratrol), whereas car-WT TTR is less amenable to resveratrol stabilization (88 ± 0.5% aggregation inhibition with respect to car-TTR without resveratrol).

The Aggregate Morphology of Oxi-TTRs Is Different from That of Nonoxidized TTRs. Transmission electron microscopy (TEM) was used to evaluate the aggregate morphology of the different TTR isoforms under acid-mediated aggregation conditions (pH 4.4, 1 day at 37 °C). Nonoxidized

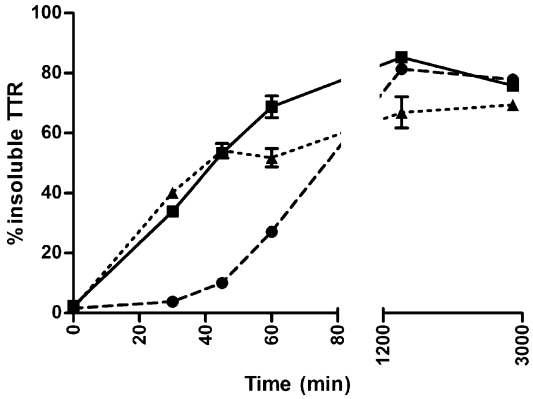

Figure 3. Kinetics of aggregation and fibril formation of monomeric M-TTR and its oxidized isoforms. Aggregation of native M-TTR (solid line, squares), oxi-M-TTR (dashed line, circles), and car-M-TTR (dotted line, triangles) was induced by incubation at pH 4.4 and 37 °C without agitation. The percentage of insoluble TTR was measured over time. Data are shown for one representative experiment performed in triplicate (mean ± SD).

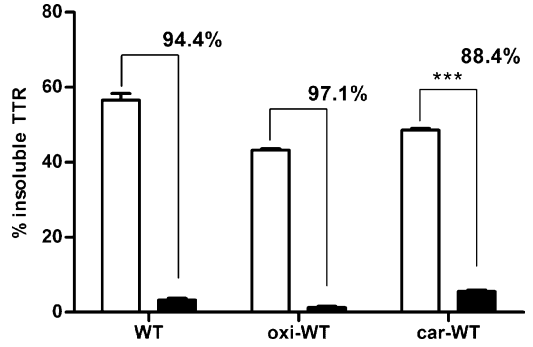

Figure 4. Resveratrol-mediated inhibition of aggregation and fibril formation. WT TTR, oxi-WT, and car-WT TTR were incubated at pH 4.4 for 3 days at 37 °C in the presence (black bars) or absence (white bars) of resveratrol. The percentage of insoluble protein was measured with respect to the initial protein content. The numbers over the bars represent the percentages of aggregation inhibition of resveratrol-containing samples with respect to vehicle-containing samples. The data show that car-WT TTR is less amenable to resveratrol-mediated inhibition of aggregation and fibril formation than native WT TTR (88% vs 94%, $p \leq 0.001$, unpaired t test).

WT and V122I TTR samples were characterized by the presence of elongated material (Figure 5a,d, arrows) as well as abundant small spherical aggregates (Figure 5a,d, circles). In contrast, samples from the oxi-TTR variants (oxi-WT and oxi-V122I TTR) were consistently richer in longer aggregates (Figure 5b,e, arrows) than those found in the nonoxidized proteins. In oxi-TTR samples, very few of the spherical aggregates were detected. Carbonylated TTR isoforms were characterized by the presence of elongated material, usually shorter than that found in nonoxidized TTRs samples (Figure 5c,f, arrows) with abundant spherical amorphous aggregates (Figure 5c,f, circles). In some of the regions of the copper grids, there were larger amorphous deposits that appeared to consist of very short, entangled, elongated structures (not shown). These structures were observed in all the samples, although they were less abundant in the oxi-TTR samples than in the native or car-TTRs samples. With longer incubation times (3 and 7 days), particularly with the faster-aggregating V122I TTR isoforms, most of the material detected was in the shape of large amorphous aggregates consisting of the same short elongated structures mentioned above, or dense deposits opaque to TEM (not shown).

Oxidative Modifications of TTR Decrease Its Thermodynamic Stability. The thermodynamic stability of oxidized and nonoxidized TTRs was studied by urea-mediated denaturation and renaturation curves at pH 7.6. As in the process of aggregation and fibril formation, the rate-limiting step for TTR unfolding in urea is the dissociation of the tetramer into its constituent monomers.[46]

The quaternary structural changes induced by urea (i.e., tetramer dissociation and tetramer reassembly) were measured by resveratrol fluorescence. The binding of resveratrol in the TTR T_4 pocket results in a sizable increase in resveratrol fluorescence that is linear with tetrameric TTR concentration.[37] Resveratrol does not bind to or fluoresce with monomeric TTR subunits, nor does it shift the monomer−tetramer equilibrium;[12] therefore, it is a useful probe for quantifying the amount of tetrameric TTR in a given solution. Standard curves using oxidized (oxi-TTRs and car-TTRs) and nonoxidized TTRs in the ranges of concentrations used for these studies (0−0.15 mg/mL) demonstrated that resveratrol fluorescence is linear with tetrameric TTR concentration (not shown).

The tertiary structural changes induced by urea (i.e., unfolding and refolding) were monitored by intrinsic tryptophan fluorescence,[37] which allows the quantification of the fraction of unfolded TTR versus folded TTR at any given urea concentration. Figure 6 shows the denaturation and renaturation curves of WT (a−d) and V122I TTR (e−h) and their oxidized isoforms. The data were fit to a sigmoidal curve, and the concentration of urea at the midpoint of denaturation or renaturation (C_m) was determined (Table 2).

For each protein, the C_m values for tetramer disassembly and reassembly (measured by resveratrol binding) are equal to or smaller than the C_m values for unfolding and refolding (measured by tryptophan fluorescence), respectively. These results are consistent with the notion that the tetramer has to first disassemble to unfold. TTR tetramer disassembly and monomer unfolding in urea is a process that takes days to reach equilibrium and is much slower than the refolding and reassembly process that takes only a few seconds.[37] In the disassembly−unfolding direction at urea concentrations of >4 M, there is still a considerable amount of tetrameric TTR (>20%), which is not present in the refolding−reassembly direction (Figure 6), indicating that for the denaturation solutions, at the time of measurement (96 h), thermodynamic equilibrium had not been reached. Longer incubation times in urea are not advisable because urea covalently modifies the proteins in a time-dependent manner.[47] Although the calculated C_m values for the denaturation and renaturation processes were very similar, for the sake of clarity we focus on the refolding−reassembly curves where thermodynamic equilibrium has been reached for all the TTR variants studied.

The data show that for both oxi-TTRs and car-TTRs the C_m values for refolding and reassembly are lower than those of their nonoxidized counterparts; these results suggest that oxi-TTRs and car-TTRs are thermodynamically less stable than native TTRs (Table 2).

For WT TTR and its oxidized variants, the C_m for refolding and the C_m for tetramer reassembly are very similar, indicating that as soon as the polypeptides refold, they assemble into tetramers. In contrast, for V122I TTR, there is a substantial difference between the C_m values for refolding and the C_m

dx.doi.org/10.1021/bi301313b | Biochemistry 2013, 52, 1913−1926

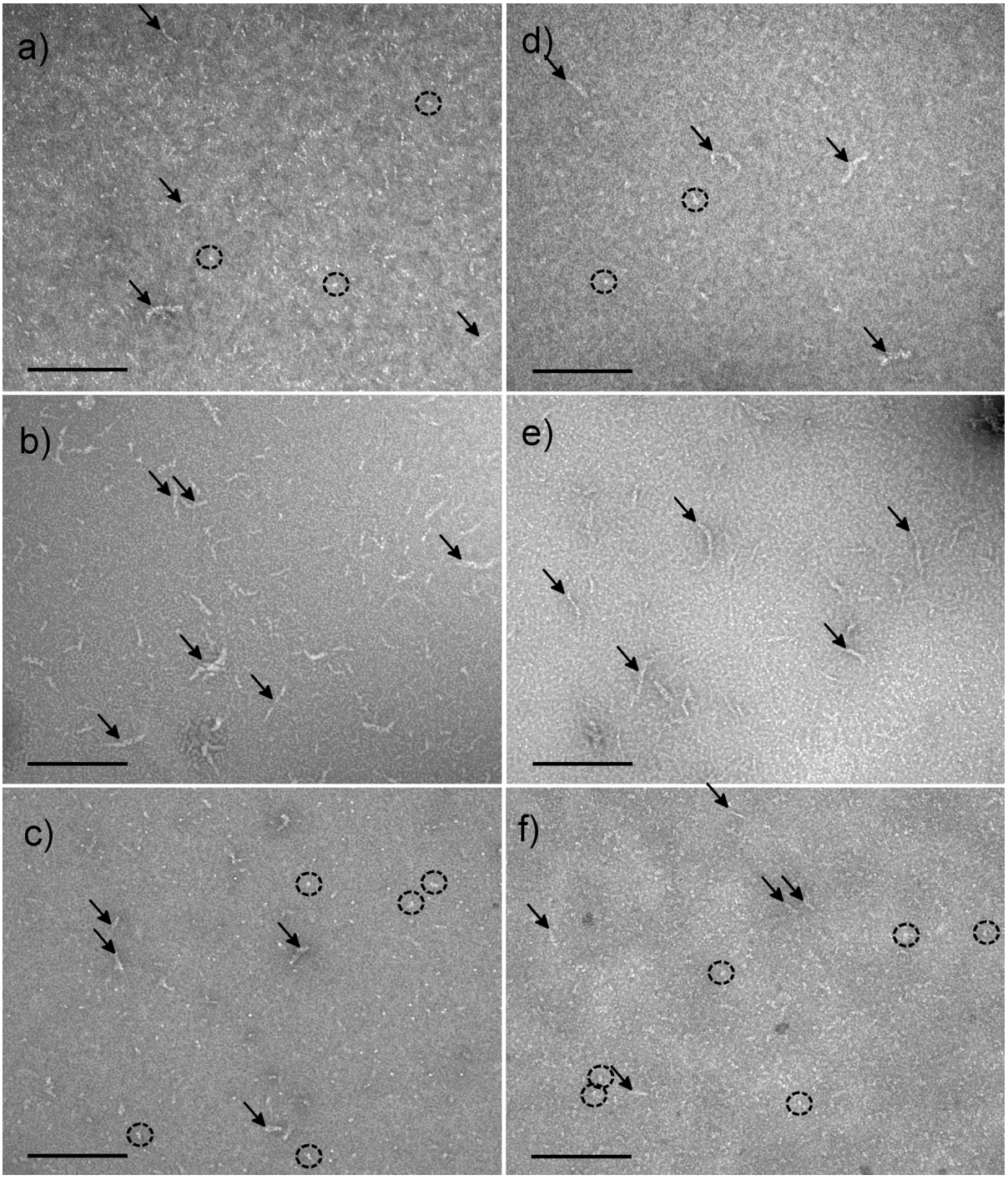

Figure 5. Negative stain TEM images of WT and V122I TTR and their oxidized isoforms subjected to acid-mediated aggregation conditions for 24 h at 37 °C: (a) WT TTR, (b) oxi-WT TTR, (c) car-WT TTR, (d) V122I TTR, (e) oxi-V122I TTR, and (f) car-V122I TTR. All images were taken at 92000× magnification. Scale bars represent 200 nm.

values for tetramer reassembly (0.5, 0.3, and 0.8 molar unit for V122I TTR, oxi-V122I TTR, and car-V122I TTR, respectively), with the C_m values for refolding being higher than those for reassembly. The C_m values for refolding of V122I and its oxidized forms are similar to the C_m values for refolding of WT and its oxidized products (~3.5, 2.8, and 3.3 M for native, oxi-TTRs, and car-TTRs, respectively). Together, these results suggest that the monomers of WT and their corresponding V122I variants have similar thermodynamic stabilities, whereas the tetramers for the WT TTR isoforms have thermodynamic stabilities higher than those of their respective V122I TTR isoforms. TTR carbonylation has a stronger effect in destabilizing the tetramer as seen by the larger differences in C_m between refolding and reassembly (0.2 and 0.8 M for car-WT and car-V122I, respectively, compared to 0.1 and 0.5 M for WT and V122I TTR, respectively).

Oxidative Modifications of TTR Change Its Kinetic Stability. We next studied the kinetic stability of the oxidized TTRs in 6 M urea, a concentration at which TTR remains irreversibly unfolded. The percentage of folded protein in

dx.doi.org/10.1021/bi301313b | *Biochemistry* 2013, 52, 1913−1926

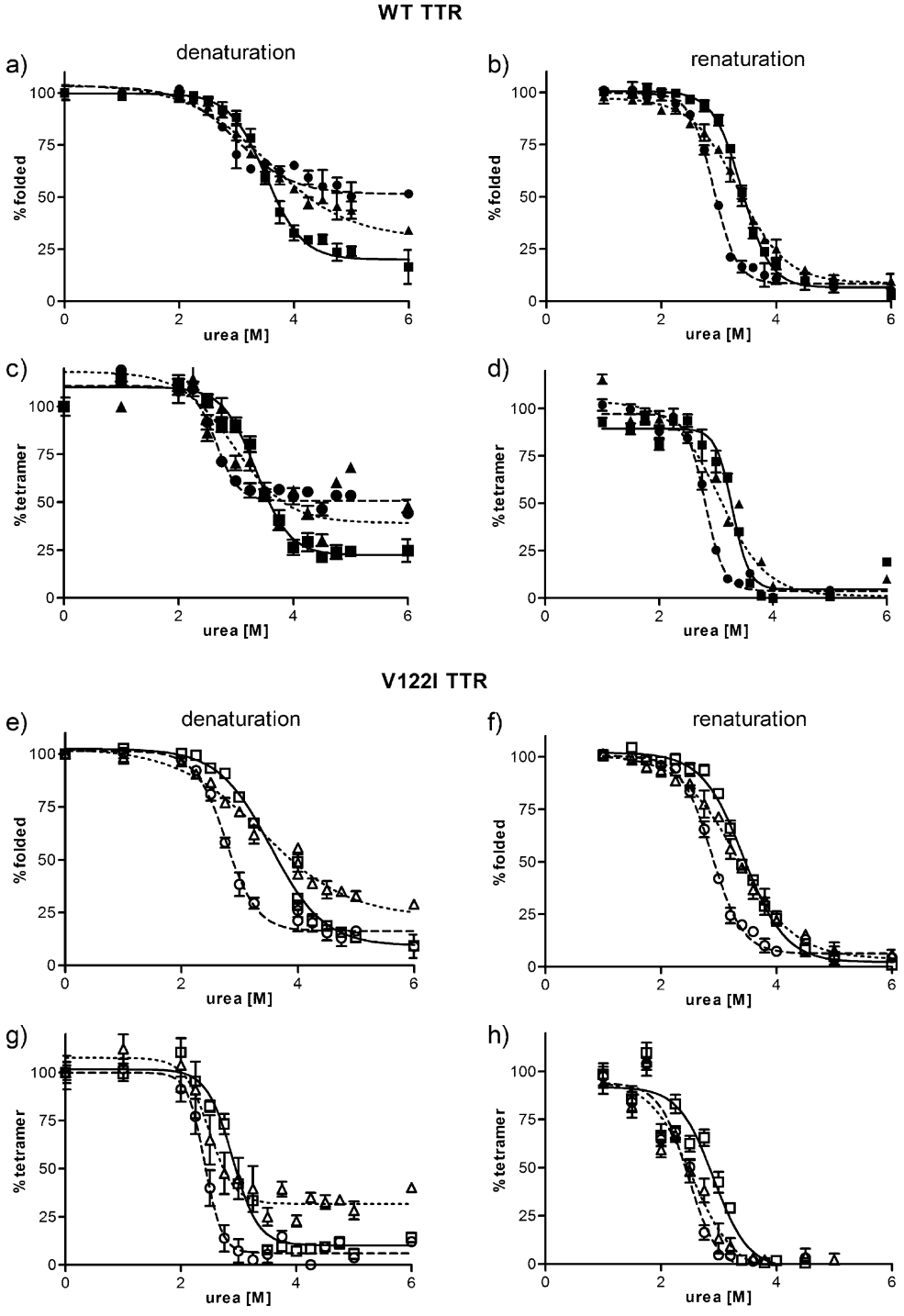

Figure 6. Stability curves of native and oxidized TTR variants in urea. WT TTR and its oxidized isoforms (a–d) and V122I and its oxidized isoforms (e–h) were incubated in the presence of various concentrations of urea. The curves were generated in the denaturation direction (a, c, e, and g) and in the renaturation direction (b, d, f, and h). The amount of folded TTR at any given urea concentration was measured by tryptophan fluorescence (a, b, e, and f), and the amount of tetrameric TTR at any given urea concentration was measured by resveratrol fluorescence (c, d, g, and h): nonoxidized TTR (solid line, squares), oxi-TTR (dashed line, circles), and car-TTR (dotted line, triangles). Data for WT TTR and its isoforms are represented by filled symbols, and data for V122I TTR and its oxidized isoforms are represented by empty symbols. Data represent the average of at least three independent experiments performed in triplicate (mean ± SD).

solution was measured over time by tryptophan fluorescence. Consistent with published results, the data show that V122I TTR in urea unfolds much faster (75% unfolded in <24 h) than WT TTR (75% unfolded in ~200 h) in urea (Figure 7), indicating a decreased kinetic stability of V122I TTR with respect to that of WT TTR.[42]

Oxi-WT TTR unfolds more slowly than native or car-WT TTRs (Figure 7). At 96 h, only ~25% of WT and car-WT remained folded, whereas more than 50% of the oxi-WT TTR was still folded. These results are consistent with an increased kinetic stability of oxi-WT TTR with respect to that of WT TTR or car-WT TTR. For V122I TTR, however, oxi-V122I

dx.doi.org/10.1021/bi301313b | *Biochemistry* 2013, 52, 1913–1926

Table 2. Midpoint Transition Values (C_m) of TTR Denaturation–Renaturation Curves in Urea[a]

	unfolding		refolding		disassembly		reassembly	
	C_m	p^b	C_m	p^b	C_m	p^b	C_m	p^b
WT	3.5 ± 0.06		3.5 ± 0.12		3.4 ± 0.09		3.4 ± 0.08	
oxi-WT	3.0 ± 0.05	****	2.8 ± 0.12	****	2.8 ± 0.19	**	2.8 ± 0.03	***
car-WT	3.4 ± 0.15	ns	3.3 ± 0.05	**	2.8 ± 0.27	**	3.1 ± 0.00	**
V122I	3.4 ± 0.06		3.4 ± 0.07		2.8 ± 0.07		2.9 ± 0.08	
oxi-V122I	2.8 ± 0.04	****	2.8 ± 0.05	****	2.4 ± 0.09	****	2.5 ± 0.05	****
car-V122I	3.4 ± 0.03	ns	3.3 ± 0.06	ns	2.5 ± 0.04	***	2.5 ± 0.02	****

[a]All C_m values are presented in molar units. TTR unfolding and refolding were measured by tryptophan fluorescence; tetramer disassembly and reassembly were measured by resveratrol binding fluorescence. [b]p values measure the significant changes in C_m for the oxidized proteins with respect to their nonoxidized counterparts. Unpaired t test: ns (not significant), $p > 0.05$; **$p \leq 0.01$; ***$p \leq 0.001$; ****$p \leq 0.0001$.

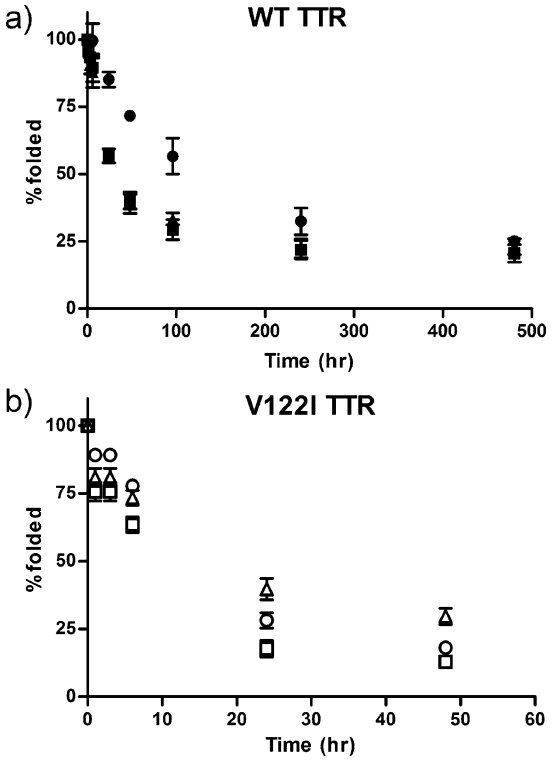

Figure 7. Kinetic stability of native and oxidized TTR variants in urea. TTR samples were incubated in 6 M urea at room temperature over 480 h. The degree of folded protein was measured by tryptophan fluorescence: (a) WT TTR (■), oxi-WT TTR (●), and car-WT TTR (▲) and (b) V122I TTR (□), oxi-V122I TTR (○), and car-V122I TTR (△). The data shown represent the average of two independent experiments performed in triplicate (mean ± SD). To appreciate the relative kinetic stabilities of V122I TTR and its oxidized isoforms, the time scale is reduced to 60 h.

unfolds at a slightly lower rate than native V122I TTR (i.e., similar kinetic stabilities). Car-V122I TTR unfolds at a lower rate than V122I TTR, indicating that it has increased kinetic stability.

Oxidized TTRs Have Cytotoxic Potencies Similar to That of Native TTRs. We have previously established tissue culture model systems for studying the TTR amyloidoses in a physiologic setting.[32,33] In these systems, we showed that amyloidogenic TTR variants such as V122I TTR and V30M TTR are cytotoxic to cells of human cardiac and neuronal origin in a dose-responsive manner,[32,33] whereas nonamyloidogenic TTR (T119M) is not.

We used the human cardiac tissue culture system to determine the cytotoxic potential of the oxidized forms of TTR with respect to their nonoxidized counterparts. AC16 cells were treated with different concentrations of WT and V122I TTR and its oxidized isoforms for 24 h at 37 °C. Cell viability was measured by the resazurin reduction assay. The results show that all oxidized TTR isoforms are cytotoxic to the human cardiac cell line AC16 in a dose-responsive manner (Figure 8); consequently, they have the potential to induce tissue damage in vivo.

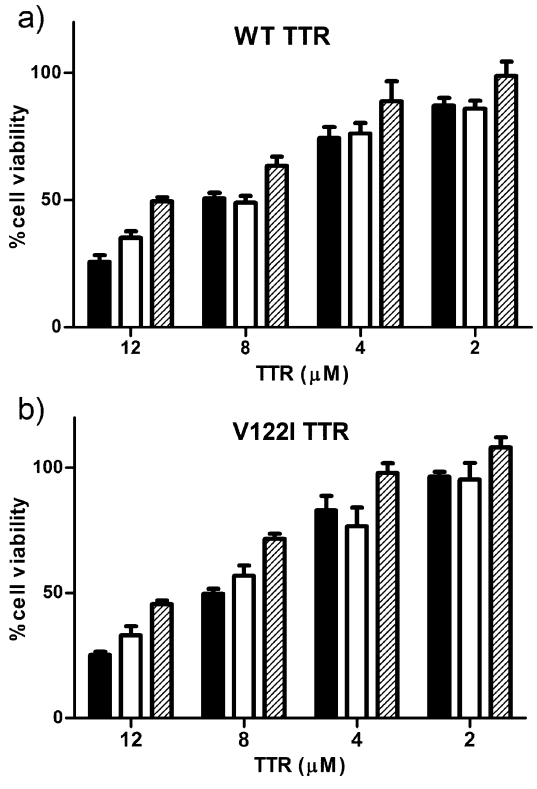

Figure 8. Cytotoxicity of WT TTR and its oxidized isoforms (a) and V122I TTR and its oxidized isoforms (b) to human cardiomyocytes. AC16 cells were exposed to several concentrations of native and oxidized TTRs for 24 h. Cell viability was measured by resazurin reduction assay. The percentage of cell viability was determined with respect to vehicle-treated samples (100% viability): native TTR, black bars; oxi-TTR, white bars; car-TTR, hatched bars. Results are representative of two independent experiments performed in quadruplicate (mean ± SD).

dx.doi.org/10.1021/bi301313b | Biochemistry 2013, 52, 1913–1926

DISCUSSION

One of the hallmarks of aging is the increased abundance of oxidized proteins in plasma and tissues. In this paper, we explore how oxidation of the plasma protein TTR could result in isoforms with increased levels of aggregation and fibril formation propensity, contributing to the onset of the senile forms of the TTR amyloidoses. We focused on WT and the V122I TTR variant because both proteins are related to late onset TTR aggregation diseases affecting the heart (SSA and FAC).

We have chosen two types of protein oxidative modifications that are relevant to the process of aging, Met/Cys oxidation and carbonylation. Far- and near-UV CD studies demonstrated that the oxidative modifications created did not alter the secondary or tertiary structure of the protein (Figure S2 of the Supporting Information). The tryptophan fluorescence spectra show identical traces for nonoxidized and oxi-TTR and a lower-intensity trace, albeit with the same maximal emission, for car-TTR. These results are not unexpected because each TTR polypeptide has 32 amino acid residues susceptible to metal-catalyzed carbonylation; some of these carbonylated residues might be spatially close to the reporting Trp residues (Trp41 and Trp79) and partially quench their fluorescence intensity. The fact that all the proteins have the same Trp fluorescence maximal emission wavelength at 335 nm indicates that the proteins are folded.

In our extensive aggregation studies from pH 4.0 to 5.88, we determined that turbidity measurements may not be a reliable measure of aggregated (insoluble) protein content. The differences are particularly striking at the lowest pH studied (pH 4.0) where very little turbidity is detected while there was a very high proportion of insoluble protein (Figure 1). Remarkably, very significant differences were also found for oxi-TTRs at the pH of maximal turbidity (4.37−4.56). At these pH values, the levels of turbidity of oxi-WT and oxi-V122I TTR are less than half of those of WT and V122I TTR, respectively, whereas oxi-WT and WT TTR, and oxi-V122I and V122I TTR, form very similar amounts of insoluble aggregates (Figure 1). TEM analysis of these TTR isoforms with different behavior at pH 4.4 can help to rationalize the discrepancy between the turbidity levels and the amount of insoluble protein detected (Figure 5). WT and V122I TTR at pH 4.4 form short fibrillar structures and small amorphous spherical aggregates, whereas in the preparations of oxi-WT and oxi-V122I TTR, we observed essentially longer fibrillar structures and almost none of the spherical aggregates (Figure 5). The concentration of particles for nonoxidized WT and V122I TTR, where high levels of turbidity are detected, is greater than for the oxi-TTR isoforms because in the former the aggregates are smaller than in the latter. Thus, turbidity appears to report on the concentration of large particles (large enough to interfere with 330−400 nm light waves) regardless of their particular size. These results are consistent with those reported by Lundberg et al.,[48] where WT TTR was aggregated over a wide pH range (2.0−5.5). The turbidity of the samples was measured, and atomic force microscopy images were recorded. The images show that at lower pH (2−3.5), where no turbidity is detected, there are large filaments whereas at higher pH (>4.0), where there is turbidity, the aggregates are small and mainly spherical.

The ThT fluorescence signal correlates quite well with the amount of insoluble protein detected (Figure 2). The TEM images show that for nonoxidized TTR both short fibrillar and amorphous aggregates are present in these solutions (Figure 5). Thus, it appears that ThT fluorescence might not be specific for amyloid fibrils but that it is sensitive to smaller amorphous aggregates as well.[11,49] It should be noted, however, that ThT fluorescence for TTR is relatively weak compared to that of other amyloidogenic peptides and proteins; therefore, there is the possibility that the apparent correlation between ThT fluorescence and insoluble aggregate formation coincides with the amount of bona fide amyloid fibrils that bind ThT. Given that the turbidity levels do not appear to represent aggregated protein under all conditions and for all TTR isoforms, we relied on insoluble protein formation for the interpretation of the results.

Consistent with our former observations,[30] oxi-TTRs form the lowest quantity of aggregates and fibrils within the entire pH range tested at earlier time points (up to 3 days for oxi-WT and up to 8 h for oxi-V122I TTR). The formation of insoluble aggregates becomes similar to those of nonoxidized TTRs and car-TTRs later in the aggregation process (Figure 1 and Figure S3 of the Supporting Information). These results suggest that oxi-TTRs might be kinetically stable with respect to native TTRs because they have slower rates of insoluble aggregate formation. The TTR denaturation studies in 6 M urea clearly show a slower rate of unfolding for oxi-WT TTR than for WT TTR. These results demonstrate that oxi-WT TTR is kinetically more stable than nonoxidized WT TTR (Figure 7). The V122I TTR isoforms are kinetically much less stable than the WT TTR isoforms, as seen by their faster unfolding rates in 6 M urea (Figure 7). In this case, we detected a slight increase in the kinetic stability of oxi-V122I with respect to that of V122I TTR. These observations are consistent with the fact that for oxi-V122I TTR, aggregation and fibril formation occur at slightly slower rates than for V122I TTR and can be detected only during the first 24 h of the aggregation process (Figure S3 of the Supporting Information).

With respect to thermodynamic stability, in the presence of urea, the calculated midpoints for tetramer reassembly (C_m) are lower for oxi-WT TTR and car-WT TTR (3.1 M) than for WT TTR (3.4 M), indicating that the oxi- and car-WT TTR are thermodynamically less stable than WT TTR. The same is true for oxi-V122I TTR and car-V122I TTR (2.5 M) with respect to V122I TTR (2.9 M) (Figure 6 and Table 2). These observations imply that at equilibrium the fraction of monomeric TTR in solution will be higher for the oxi-TTRs and car-TTRs than for their nonoxidized counterparts; thus, the oxidized proteins will be more prone to aggregation and deposition in vivo.

The TTR aggregation propensity depends on a combination of both thermodynamic and kinetic stability parameters.[13] Oxi-TTRs have the potential to be more amyloidogenic than native TTRs as seen by the lower thermodynamic stability of the tetramer. It is possible, however, that their enhanced kinetic stability slows the dissociation of the tetramer in vivo and, thus, decreases the rate of the overall TTR aggregation process.

Carbonylated WT and V122I TTR have higher aggregation propensities than their nonoxidized counterparts at pH values closer to physiological (4.88 and 5.13). Car-TTRs are also thermodynamically less stable than native TTRs as seen by the lower C_m values for refolding and particularly those for tetramer reassembly in urea (Figure 6 and Table 2). Moreover, it appears that car-TTRs have a kinetic stability similar to those of nonoxidized TTRs (Figure 7). Together, these results suggest that in vivo, car-TTRs will have a higher tendency to aggregate

and deposit than nonoxidized TTRs and contribute to the onset of the senile forms of the TTR amyloidoses. We hypothesize that a decrease in the thermodynamic stability of TTR (in the absence of a change in kinetic stability) results in aggregation and fibril formation at higher pH values in vitro and the development of amyloid deposition in vivo. This notion is supported by other cases found in the literature. For example, the V30M TTR variant, related to FAP, is thermodynamically unstable (C_m in urea of 2.0 M, compared to 3.4 M for WT TTR), while its pH of maximal fibril formation is 5.2 (compared to 4.4 for WT TTR).[50] Other TTR variants such as L58H and I84S TTR, for which both thermodynamic stability parameters (both have a C_m of 2.4 M in urea) and the pH of maximal fibril formation (pH 4.8−4.9) have been reported, follow the same trend.[50] Only the T60A TTR variant appears to be an exception to this trend (C_m of 2.8 M and pH of maximal fibril formation of 4.5). Further support for this hypothesis is found in Zhang et al.,[51] where the stability and fibril formation propensity of Cys10-modified TTR variants were characterized. They report that TTR variants that are thermodynamically less stable than WT TTR form fibrils over a higher pH range, whereas one of the variants that forms the maximal amount of fibrils and aggregates at the same pH as WT TTR had the same thermodynamic stability.[51] It is not known, however, whether these variants are involved in early onset amyloid disease.

Aggregation studies performed using the well-characterized engineered monomeric TTR (M-TTR)[44] and its oxidized isoforms show that oxi-M-TTR aggregates at a slower rate than nonoxidized M-TTR, suggesting that it might also be kinetically more stable (Figure 3), yet the rates of aggregation of tetramer TTRs are much slower than those of monomeric TTRs, indicating that even with oxidized proteins the rate-limiting step in the aggregation process is the dissociation of the tetramer. The slower aggregation rate of oxi-M-TTR with respect to that of M-TTR could also be explained by the fact that the former is more hydrophilic than the latter, as seen by faster elution times in a high-performance liquid chromatography column in reverse phase (not shown). It is known that protein aggregation is driven by hydrophobic interactions; thus, the decrease in hydrophobicity of oxi-M-TTR with respect to that of M-TTR could also contribute to the observed slower aggregation rate. These results are consistent with the decreased fibril formation propensities of the MetO Aβ peptide,[52] prion protein,[53] α-synuclein,[54] and apolipoprotein C-II[55] with respect to those of their nonoxidized counterparts.

In conclusion, the age-related oxidative modifications of TTR studied decrease the protein's thermodynamic stability and can therefore have an impact on the onset of the senile forms of the TTR amyloidoses in vivo. Although oxi-WT TTR is kinetically more stable than nonoxidized TTR, it still forms the same quantity of aggregates at sufficiently long time points (>7 days). It is unknown how these two parameters, thermodynamic and kinetic stability, will play in vivo. However, other TTR variants with extremely high kinetic stability such as Y69H and F64S TTR and low thermodynamic stability are known to be amyloidogenic in vivo.[13]

The current treatment for TTR amyloidosis related to deposition of mutant TTR is liver transplantation. In this procedure, the mutant TTR-producing liver is replaced by a wild-type TTR-producing liver.[56] More recently, a new pharmacologic-based therapeutic strategy is undergoing human clinical trials and is already approved in Europe for the treatment of early stage TTR amyloidosis.[57,58] This strategy consists of the administration of small molecules that by binding in the TTR T_4 pocket kinetically stabilize the native tetramer and prevent aggregation and fibril formation.[57,59] Resveratrol is one such molecule with a high capacity to kinetically stabilize tetrameric TTR and prevent aggregation in vitro[45] and TTR-induced toxicity in tissue culture.[32,33] By binding in the TTR T_4 pocket, resveratrol precludes the dissociation of the TTR tetramer into its corresponding monomers, the precursors of the fibrils and aggregates. Our studies show that car-WT TTR was less amenable to resveratrol-mediated tetramer stabilization than nonoxidized WT TTR (Figure 4). The TTR T_4 binding pocket contains residues that are susceptible to carbonyl modification (Lys15 and Thr119). It is possible that such modification results in a decreased affinity of resveratrol for the TTR T_4 binding pocket. These results suggest that for the senile forms of the TTR amyloidoses, in which an increased amount of carbonylated TTR might be present, kinetic stabilization of the tetramer by small molecules might be less effective than in cases of early onset disease associated with more aggressive but nonoxidized TTR mutants. Thus, a therapeutic strategy to delay the onset of the senile forms of the TTR amyloidoses should consider the prevention of oxidative carbonylation of TTR.

In mouse models of the TTR amyloidoses and in human biopsies of asymptomatic mutant TTR carriers, there is evidence of tissue damage and cell death well before there is detectable TTR deposition.[31] We have previously established a tissue culture model system for the TTR amyloidoses using human-derived cardiomyocytes of the ventricle, the site of TTR deposition in the heart.[32] In this system, amyloidogenic TTR variants are toxic to the AC16 human cardiomyocytes, whereas the stable and nonamyloidogenic T119M TTR is not. Herein, we show that all the oxidized forms of TTR are toxic to AC16 human cardiomyocytes in a dose-responsive manner (Figure 8), indicating that, like their nonoxidized counterparts, they have potential for tissue damage, before deposition occurs.

In summary, our studies show that an increase in the level of the oxidative state of TTR due to aging might be a factor contributing to the onset of the TTR amyloidoses. The decreased capacity of resveratrol to stabilize carbonylated WT TTR suggests that additional therapeutic strategies for tetramer stabilization, such as antioxidant therapy, might be required to delay or prevent the onset of the senile forms of the TTR systemic amyloidoses.

■ ASSOCIATED CONTENT

Supporting Information

Analysis of carbonyl TTRs by Western blots (Figure S1), far- and near-UV CD spectra and tryptophan fluorescence spectra of WT TTR and V122I TTR and their oxidized isoforms (Figure S2), and kinetics of aggregation and fibril formation of WT and V122I TTR and their oxidized isoforms at pH 4.4 measured by turbidity and insoluble protein content (Figure S3). This material is available free of charge via the Internet at http://pubs.acs.org.

■ AUTHOR INFORMATION

Corresponding Author

*Phone: (858) 784-8893. Fax: (858) 784-8891. E-mail: natalia@scripps.edu.

Funding

This research was supported by the National Institutes of Health (National Institute on Aging Grant AG032285 to N.R.) and the American Heart Association (Grant 0865061F to N.R.).

Notes

The authors declare no competing financial interest.

■ ACKNOWLEDGMENTS

We thank Dr. Malcolm R. Wood (The Scripps Research Institute) for the acquisition of the TEM images, Jeanine Witkowski for preparing and purifying some of the recombinant protein used for these studies, Dr. Mercy Davidson (Columbia University, New York, NY) for providing the AC16 cells,[38] Dr. Lawreen H. Connors (Boston University, Boston, MA) for generously providing the rTTR plasmid,[34] and Dr. Jeffery W. Kelly for allowing us to use some of the instruments in his laboratory. We also thank Dr. Jaime Pascual and Dr. R. Luke Wiseman for carefully reading the manuscript.

■ ABBREVIATIONS

CD, circular dichroism; CSF, cerebrospinal fluid; Cys-SO_3H, Cys sulfonic acid; FAC, familial amyloid cardiomyopathy; GndCl, guanidinium chloride; GF buffer, 10 mM sodium phosphate (pH 7.6), 100 mM KCl, and 1 mM EDTA buffer; H_2O_2, hydrogen peroxide; HBSS, Hank's Balanced Salt Solution; LC−MS, liquid chromatography-mass spectrometry; MetO, methionine sulfoxide; rTTR, recombinant transthyretin lacking Met at position −1; SD, standard deviation; SSA, senile systemic amyloidosis; T_4, thyroxine; TEM, transmission electron microscopy; ThT, thioflavin T; TTR, transthyretin; V122I TTR, Val122IIe TTR; WT TTR, wild-type TTR.

■ REFERENCES

(1) Buxbaum, J. N. (2004) The systemic amyloidoses. *Curr. Opin. Rheumatol. 16*, 67−75.
(2) Sipe, J. D., Benson, M. D., Buxbaum, J. N., Ikeda, S., Merlini, G., Saraiva, M. J., and Westermark, P. (2010) Amyloid fibril protein nomenclature: 2010 recommendations from the nomenclature committee of the International Society of Amyloidosis. *Amyloid 17*, 101−104.
(3) Li, X., Masliah, E., Reixach, N., and Buxbaum, J. N. (2011) Neuronal production of transthyretin in human and murine Alzheimer's disease: Is it protective? *J. Neurosci. 31*, 12483−12490.
(4) Buxbaum, J. N., and Reixach, N. (2009) Transthyretin: The servant of many masters. *Cell. Mol. Life Sci. 66*, 3095−3101.
(5) Cornwell, G. G., III, Murdoch, W. L., Kyle, R. A., Westermark, P., and Pitkanen, P. (1983) Frequency and distribution of senile cardiovascular amyloid. A clinicopathologic correlation. *Am. J. Med. 75*, 618−623.
(6) Tanskanen, M., Peuralinna, T., Polvikoski, T., Notkola, I. L., Sulkava, R., Hardy, J., Singleton, A., Kiuru-Enari, S., Paetau, A., Tienari, P. J., and Myllykangas, L. (2008) Senile systemic amyloidosis affects 25% of the very aged and associates with genetic variation in α2-macroglobulin and tau: A population-based autopsy study. *Ann. Med. 40*, 232−239.
(7) Jacobson, D. R., Pastore, R., Pool, S., Malendowicz, S., Kane, I., Shivji, A., Embury, S. H., Ballas, S. K., and Buxbaum, J. N. (1996) Revised transthyretin Ile 122 allele frequency in African-Americans. *Hum. Genet. 98*, 236−238.
(8) Buxbaum, J., Jacobson, D. R., Tagoe, C., Alexander, A., Kitzman, D. W., Greenberg, B., Thaneemit-Chen, S., and Lavori, P. (2006) Transthyretin V122I in African Americans with congestive heart failure. *J. Am. Coll. Cardiol. 47*, 1724−1725.
(9) Jacobson, D. R., Pastore, R. D., Yaghoubian, R., Kane, I., Gallo, G., Buck, F. S., and Buxbaum, J. N. (1997) Variant-sequence transthyretin (isoleucine 122) in late-onset cardiac amyloidosis in black Americans. *N. Engl. J. Med. 336*, 466−473.
(10) Kelly, J. W. (1998) The alternative conformations of amyloidogenic proteins and their multi-step assembly pathways. *Curr. Opin. Struct. Biol. 8*, 101−106.
(11) Hurshman, A. R., White, J. T., Powers, E. T., and Kelly, J. W. (2004) Transthyretin aggregation under partially denaturing conditions is a downhill polymerization. *Biochemistry 43*, 7365−7381.
(12) Hammarstrom, P., Jiang, X., Hurshman, A. R., Powers, E. T., and Kelly, J. W. (2002) Sequence-dependent denaturation energetics: A major determinant in amyloid disease diversity. *Proc. Natl. Acad. Sci. U.S.A. 99* (Suppl. 4), 16427−16432.
(13) Sekijima, Y., Wiseman, R. L., Matteson, J., Hammarstrom, P., Miller, S. R., Sawkar, A. R., Balch, W. E., and Kelly, J. W. (2005) The biological and chemical basis for tissue-selective amyloid disease. *Cell 121*, 73−85.
(14) Stadtman, E. R. (2006) Protein oxidation and aging. *Free Radical Res. 40*, 1250−1258.
(15) Stadtman, E. R., and Levine, R. L. (2003) Free radical-mediated oxidation of free amino acids and amino acid residues in proteins. *Amino Acids 25*, 207−218.
(16) Fedorova, M., Kuleva, N., and Hoffmann, R. (2010) Identification of cysteine, methionine and tryptophan residues of actin oxidized in vivo during oxidative stress. *J. Proteome Res. 9*, 1598−1609.
(17) Poole, L. B. (2004) Formation and functions of protein sulfenic acids. *Current Protocols in Toxicology*, Chapter 17, Unit 17, Wiley, New York.
(18) Hoshi, T., and Heinemann, S. (2001) Regulation of cell function by methionine oxidation and reduction. *J. Physiol. 531*, 1−11.
(19) Shacter, E. (2000) Quantification and significance of protein oxidation in biological samples. *Drug Metab. Rev. 32*, 307−326.
(20) Amici, A., Levine, R. L., Tsai, L., and Stadtman, E. R. (1989) Conversion of amino acid residues in proteins and amino acid homopolymers to carbonyl derivatives by metal-catalyzed oxidation reactions. *J. Biol. Chem. 264*, 3341−3346.
(21) Dalle-Donne, I., Rossi, R., Giustarini, D., Milzani, A., and Colombo, R. (2003) Protein carbonyl groups as biomarkers of oxidative stress. *Clin. Chim. Acta 329*, 23−38.
(22) Levine, R. L. (2002) Carbonyl modified proteins in cellular regulation, aging, and disease. *Free Radical Biol. Med. 32*, 790−796.
(23) Conrad, C. C., Marshall, P. L., Talent, J. M., Malakowsky, C. A., Choi, J., and Gracy, R. W. (2000) Oxidized proteins in Alzheimer's plasma. *Biochem. Biophys. Res. Commun. 275*, 678−681.
(24) Choi, J., Malakowsky, C. A., Talent, J. M., Conrad, C. C., and Gracy, R. W. (2002) Identification of oxidized plasma proteins in Alzheimer's disease. *Biochem. Biophys. Res. Commun. 293*, 1566−1570.
(25) Floor, E., and Wetzel, M. G. (1998) Increased protein oxidation in human substantia nigra pars compacta in comparison with basal ganglia and prefrontal cortex measured with an improved dinitrophenylhydrazine assay. *J. Neurochem. 70*, 268−275.
(26) Madian, A. G., and Regnier, F. E. (2010) Profiling carbonylated proteins in human plasma. *J. Proteome Res. 9*, 1330−1343.
(27) Guidi, F., Magherini, F., Gamberi, T., Bini, L., Puglia, M., Marzocchini, R., Ranaldi, F., Modesti, P. A., Gulisano, M., and Modesti, A. (2011) Plasma protein carbonylation and physical exercise. *Mol. BioSyst. 7*, 640−650.
(28) D'Aguanno, S., Franciotta, D., Lupisella, S., Barassi, A., Pieragostino, D., Lugaresi, A., Centonze, D., D'Eril, G. M., Bernardini, S., Federici, G., and Urbani, A. (2010) Protein profiling of Guillain-Barre syndrome cerebrospinal fluid by two-dimensional electrophoresis and mass spectrometry. *Neurosci. Lett. 485*, 49−54.
(29) Ando, Y., Nyhlin, N., Suhr, O., Holmgren, G., Uchida, K., el Sahly, M., Yamashita, T., Terasaki, H., Nakamura, M., Uchino, M., and Ando, M. (1997) Oxidative stress is found in amyloid deposits in systemic amyloidosis. *Biochem. Biophys. Res. Commun. 232*, 497−502.

(30) Maleknia, S. D., Reixach, N., and Buxbaum, J. N. (2006) Oxidation inhibits amyloid fibril formation of transthyretin. *FEBS J. 273*, 5400−5406.
(31) Sousa, M. M., Fernandes, R., Palha, J. A., Taboada, A., Vieira, P., and Saraiva, M. J. (2002) Evidence for early cytotoxic aggregates in transgenic mice for human transthyretin Leu55Pro. *Am. J. Pathol. 161*, 1935−1948.
(32) Bourgault, S., Choi, S., Buxbaum, J. N., Kelly, J. W., Price, J. L., and Reixach, N. (2011) Mechanisms of transthyretin cardiomyocyte toxicity inhibition by resveratrol analogs. *Biochem. Biophys. Res. Commun. 410*, 707−713.
(33) Reixach, N., Deechongkit, S., Jiang, X., Kelly, J. W., and Buxbaum, J. N. (2004) Tissue damage in the amyloidoses: Transthyretin monomers and nonnative oligomers are the major cytotoxic species in tissue culture. *Proc. Natl. Acad. Sci. U.S.A. 101*, 2817−2822.
(34) Kingsbury, J. S., Klimtchuk, E. S., Theberge, R., Costello, C. E., and Connors, L. H. (2007) Expression, purification, and in vitro cysteine-10 modification of native sequence recombinant human transthyretin. *Protein Expression Purif. 53*, 370−377.
(35) Noble, R. W., and Gibson, Q. H. (1970) The reaction of ferrous horseradish peroxidase with hydrogen peroxide. *J. Biol. Chem. 245*, 2409−2413.
(36) Maisonneuve, E., Ducret, A., Khoueiry, P., Lignon, S., Longhi, S., Talla, E., and Dukan, S. (2009) Rules governing selective protein carbonylation. *PLoS One 4*, e7269.
(37) Reixach, N., Foss, T. R., Santelli, E., Pascual, J., Kelly, J. W., and Buxbaum, J. N. (2007) Human-murine transthyretin heterotetramers are kinetically stable and non-amyloidogenic: A lesson in the generation of transgenic models of diseases involving oligomeric proteins. *J. Biol. Chem. 283*, 2098−2107.
(38) Davidson, M. M., Nesti, C., Palenzuela, L., Walker, W. F., Hernandez, E., Protas, L., Hirano, M., and Isaac, N. D. (2005) Novel cell lines derived from adult human ventricular cardiomyocytes. *J. Mol. Cell. Cardiol. 39*, 133−147.
(39) Stadtman, E. R., Van, R. H., Richardson, A., Wehr, N. B., and Levine, R. L. (2005) Methionine oxidation and aging. *Biochim. Biophys. Acta 1703*, 135−140.
(40) Lai, Z., McCulloch, J., Lashuel, H. A., and Kelly, J. W. (1997) Guanidine hydrochloride-induced denaturation and refolding of transthyretin exhibits a marked hysteresis: Equilibria with high kinetic barriers. *Biochemistry 36*, 10230−10239.
(41) Colon, W., and Kelly, J. W. (1992) Partial denaturation of transthyretin is sufficient for amyloid fibril formation in vitro. *Biochemistry 31*, 8654−8660.
(42) Jiang, X., Buxbaum, J. N., and Kelly, J. W. (2001) The V122I cardiomyopathy variant of transthyretin increases the velocity of rate-limiting tetramer dissociation, resulting in accelerated amyloidosis. *Proc. Natl. Acad. Sci. U.S.A. 98*, 14943−14948.
(43) LeVine, H., III (1999) Quantification of β-sheet amyloid fibril structures with thioflavin T. *Methods Enzymol. 309*, 274−284.
(44) Jiang, X., Smith, C. S., Petrassi, H. M., Hammarstrom, P., White, J. T., Sacchettini, J. C., and Kelly, J. W. (2001) An engineered transthyretin monomer that is nonamyloidogenic, unless it is partially denatured. *Biochemistry 40*, 11442−11452.
(45) Klabunde, T., Petrassi, H. M., Oza, V. B., Raman, P., Kelly, J. W., and Sacchettini, J. C. (2000) Rational design of potent human transthyretin amyloid disease inhibitors. *Nat. Struct. Biol. 7*, 312−321.
(46) Hammarstrom, P., Jiang, X., Deechongkit, S., and Kelly, J. W. (2001) Anion shielding of electrostatic repulsions in transthyretin modulates stability and amyloidosis: Insight into the chaotrope unfolding dichotomy. *Biochemistry 40*, 11453−11459.
(47) Bennion, B. J., and Daggett, V. (2003) The molecular basis for the chemical denaturation of proteins by urea. *Proc. Natl. Acad. Sci. U.S.A. 100*, 5142−5147.
(48) Lundberg, E., Olofsson, A., Westermark, G. T., and Sauer-Eriksson, A. E. (2009) Stability and fibril formation properties of human and fish transthyretin, and of the *Escherichia coli* transthyretin-related protein. *FEBS J. 276*, 1999−2011.
(49) Lindgren, M., Sorgjerd, K., and Hammarstrom, P. (2005) Detection and characterization of aggregates, prefibrillar amyloidogenic oligomers, and protofibrils using fluorescence spectroscopy. *Biophys. J. 88*, 4200−4212.
(50) Miller, S. R., Sekijima, Y., and Kelly, J. W. (2004) Native state stabilization by NSAIDs inhibits transthyretin amyloidogenesis from the most common familial disease variants. *Lab. Invest. 84*, 545−552.
(51) Zhang, Q., and Kelly, J. W. (2003) Cys10 mixed disulfides make transthyretin more amyloidogenic under mildly acidic conditions. *Biochemistry 42*, 8756−8761.
(52) Hou, L., Kang, I., Marchant, R. E., and Zagorski, M. G. (2002) Methionine 35 oxidation reduces fibril assembly of the amyloid Aβ-(1−42) peptide of Alzheimer's disease. *J. Biol. Chem. 277*, 40173−40176.
(53) Breydo, L., Bocharova, O. V., Makarava, N., Salnikov, V. V., Anderson, M., and Baskakov, I. V. (2005) Methionine oxidation interferes with conversion of the prion protein into the fibrillar proteinase K-resistant conformation. *Biochemistry 44*, 15534−15543.
(54) Uversky, V. N., Yamin, G., Souillac, P. O., Goers, J., Glaser, C. B., and Fink, A. L. (2002) Methionine oxidation inhibits fibrillation of human α-synuclein in vitro. *FEBS Lett. 517*, 239−244.
(55) Binger, K. J., Griffin, M. D., and Howlett, G. J. (2008) Methionine oxidation inhibits assembly and promotes disassembly of apolipoprotein C-II amyloid fibrils. *Biochemistry 47*, 10208−10217.
(56) Herlenius, G., Wilczek, H. E., Larsson, M., and Ericzon, B. G. (2004) Ten years of international experience with liver transplantation for familial amyloidotic polyneuropathy: Results from the Familial Amyloidotic Polyneuropathy World Transplant Registry. *Transplantation 77*, 64−71.
(57) Coelho, T., Maia, L. F., Martins da, S. A., Waddington, C. M., Plante-Bordeneuve, V., Lozeron, P., Suhr, O. B., Campistol, J. M., Conceicao, I. M., Schmidt, H. H., Trigo, P., Kelly, J. W., Labaudiniere, R., Chan, J., Packman, J., Wilson, A., and Grogan, D. R. (2012) Tafamidis for transthyretin familial amyloid polyneuropathy: A randomized, controlled trial. *Neurology 79*, 785−792.
(58) Bulawa, C. E., Connelly, S., Devit, M., Wang, L., Weigel, C., Fleming, J. A., Packman, J., Powers, E. T., Wiseman, R. L., Foss, T. R., Wilson, I. A., Kelly, J. W., and Labaudiniere, R. (2012) Tafamidis, a potent and selective transthyretin kinetic stabilizer that inhibits the amyloid cascade. *Proc. Natl. Acad. Sci. U.S.A. 109*, 9629−9634.
(59) Berk, J. L., Suhr, O. B., Sekijima, Y., Yamashita, T., Heneghan, M., Zeldenrust, S. R., Ando, Y., Ikeda, S., Gorevic, P., Merlini, G., Kelly, J. W., Skinner, M., Bisbee, A. B., Dyck, P. J., and Obici, L. (2012) The Diflunisal Trial: Study accrual and drug tolerance. *Amyloid 19* (Suppl. 1), 37−38.